A parallel, multiscale domain decomposition method for the transient dynamic analysis of assemblies with friction

David Odièvre, Pierre-Alain Boucard, Fabrice Gatuingt

A parallel, multiscale domain decomposition method for the transient dynamic analysis of assemblies with friction

D. Odièvre, P.-A. Boucard, F. Gatuingt

LMT-Cachan (ENS Cachan/CNRS/Université Paris 6/PRES UniverSud Paris)
61 av. du Président Wilson, F-94230 Cachan, France

Abstract

The objective of this work is to develop an efficient strategy for dynamic problems with multiple contacts. Our approach is based on the multiscale LATIN method with domain decomposition. This is a mixed method which deals simultaneously with the forces and velocities at the interfaces of the different subdomains. This strategy has already been applied successfully to a variety of static problems; here, it is extended to dynamics. First, we show how the multiscale strategy can be extended to dynamics. Then, we illustrate the capabilities of the method through a 3D academic example and the simulation of a heterogeneous material.

Key words: multiscale computational method, transient dynamics, domain decomposition, contact, friction, parallel processing

1 Introduction

Modeling and simulation play an important role in engineering and design departments and raise multiple problems, particularly in dynamics when dealing with large assemblies with connections. These connections have significant impact on the dimensioning process because they are subject to highly nonlinear local phenomena (contact and friction) which are even more important in fast transient dynamic problems and require very fine meshes in order to be represented correctly (1). Therefore, the choice of an efficient computational method is of vital importance.

In recent years, a number of methods based on domain decomposition procedures for the resolution of dynamic equilibrium equations have been proposed in the literature (2; 3). These methods enable one to reduce both computation

costs and the memory requirements for storing the data (thanks to parallel processing). One of the methods often used to deal with such problems in dynamics is the dual substructuring method: Lagrange multipliers are used to enforce the kinematic continuity of the primary field across the interfaces defined by the subdomain boundaries; the interface problem, which, in this case is a Schur complement operator defined on the dual variable (the Lagrange multiplier), is solved first; then, using the Lagrange multipliers thus obtained, the resolution within each subdomain leads to the interior degrees of freedom. An important dual domain decomposition method is the Finite Element Tearing and Interconnecting (FETI) method, which was initially developed by Farhat and Roux for static problems (4). Subsequently, this method was extended to transient problems in (5), to parallel processing in (6) and to frictional contact problems (7; 8). The original FETI method is also known as the single-level method. Later, the single-level FETI algorithms were extended, leading to the two-level FETI methods (9) and to the dual-primal FETI method (FETI-DP) (10). Regarding time-dependent problems, coarse problems were introduced in (11) and specific preconditioners were developed in (12) to improve the convergence rate of the method in dynamics. The dual substructuring method can also be associated with multispace-multiscale methods: for example, in (13), this algorithm, used jointly with multigrid methods (14), takes different space scales into account. In this paper, we focus on the case of assemblies of elastic structures connected through frictional contact conditions. Contact problems are characterized by constraints such as non-penetration conditions, and an active area of contact - *i.e.* the area where contact actually occurs - which is *a priori* unknown. For these reasons, such problems lead to stiff systems of nonlinear equations. There are several approaches to the resolution of static contact problems (15; 16; 17). In most of these approaches, the numerical methods used to enforce the contact constraints can be categorized into Lagrange multiplier methods and penalty methods (18). Penalty methods (19; 20) are closely related to the regularization of the contact constraints and are usually formulated in terms of the displacement variables, *i.e.* they are primal methods. These methods, an example of which is the joint finite element method (21), enable contact to be treated as a special type of material behavior. Penalty methods lead themselves to various numerical difficulties, especially ill-conditioning, when too large or too small a penalty parameter is introduced. Lagrange multiplier methods are dual methods in which the multipliers, which represent the reaction forces at the contact points, are introduced in order to enforce the non-penetration conditions strictly. Augmented Lagrange multiplier methods (22; 23; 24; 25) result in mixed formulations involving both displacement and force unknowns. The numerical resolution schemes underlying both Lagrange multiplier methods and augmented Lagrange multiplier methods are often related to the Uzawa algorithm (26; 27; 28).

The objective of the present work is to develop a specific method to deal with

the problems arising from the fact that the nonlinearities are localized in the connections, as described previously. Our approach is based on a decomposition of the assembly into substructures and interfaces. The problem is solved in each substructure using the finite element method. An iterative scheme based on the multiscale LArge Time INcrement (LATIN) method developed at the LMT Cachan (29; 30) is used for the global resolution. This approach leads to a very significant reduction in computation cost for quasi-static problems. The multiscale LATIN method is a mixed method which deals simultaneously with both velocities and forces at the interfaces and solves a homogenized macroscopic problem in order to accelerate the convergence of the numerical scheme. When only static cases are considered, the LATIN method (without the multiscale approach) can be derived by other means, such as in Lions (31) or Glowinski and Le Tallec (32). While this method has already been largely developed in statics and quasi-statics, the objective of the work presented here concerns its extension to dynamics.

2 The multiscale LATIN method

This multiscale domain decomposition method consists of three components: spatial domain decomposition, separation of the scales, and a resolution algorithm. The main features of these three components are developed below. The details of the method itself can be found in (33).

2.1 Decomposition into substructures and interfaces

An assembly is a set of substructures which communicate with one another through interfaces (See Figures 1(a) and 1(b)). Each interface represents a connection. The substructures and interfaces have their own variables and equations (admissibility, equilibrium and behavior). Two connected substructures are denoted Ω_E and $\Omega_{E'}$ and the associated interface is designated by $\Gamma_{EE'}$.

Each interface is a mechanical entity with its own variables and its specific behavior, which depends on the type of connection. Many different types of connections, such as frictional contact, can be modeled with this approach. The interface variables consist of two force fields F_E, $F_{E'}$ and two dual velocity fields W_E, $W_{E'}$ (See Figure 1(b)). By convention, F_E and $F_{E'}$ represent the action of the interface on the substructures, and W_E and $W_{E'}$ are the velocities of the substructures viewed from the interface. Thus, the interface concept can be easily extended to the boundary, where the displacements, the velocities or the forces are prescribed.
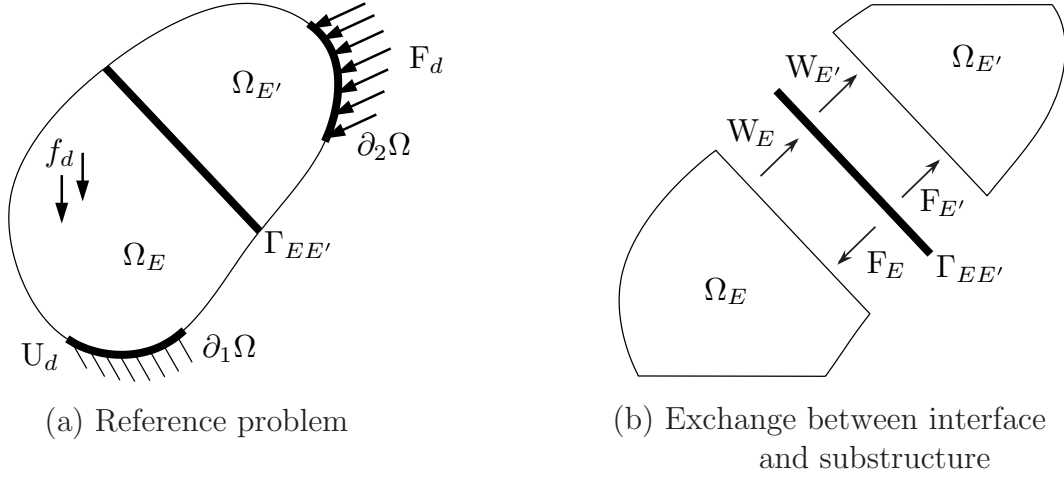
(a) Reference problem

(b) Exchange between interface and substructure

Fig. 1. Decomposition of the reference problem into substructures and interfaces

2.2 Multiscale extension

In order to ensure the theoretical scalability of the method, our approach introduces a spatial description of the unknowns on two scales, called the macroscale and the microscale. In this multiscale strategy, the interfaces play an important role of scale separation: the definitions of the microscopic and macroscopic fields are related to the interface quantities of the substructured problem and are expressed prior to any discretization.

Let us consider an interface $\Gamma_{EE'}$ whose unknowns (W_E, F_E) are divided into

$$W_E = W_E^m + W_E^M \qquad \text{and} \qquad F_E = F_E^m + F_E^M$$

where W^M and W^m denote respectively the macro parts and the micro complements of the velocity field. The separation of the two scales is obtained by means of the projection operator $\Pi_{\Gamma_{EE'}}$ defined for each interface. Over $\Gamma_{EE'}$, we write W^M and F^M in the form $X^M = \sum (X, e_i^M) e_i^M = \Pi_{\Gamma_{EE'}} X$. The choice of the macroscopic projector influences the efficiency of the algorithm. The problem of the selection of the optimum projector was studied in (30). The basis functions $\{e_i^M\}$ for a 2D problem are represented in Figure 2. The macroscopic kinematics which results from this choice consists of two translations, one rotation and one strain.
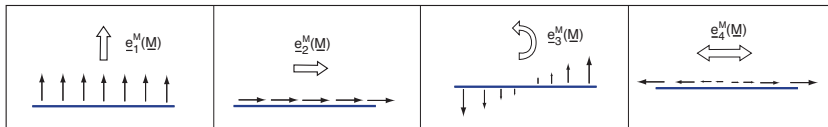

Fig. 2. The affine basis functions $\{e_i^M\}$ of an interface $\Gamma_{EE'}$

2.3 The substructured problem

■ The problem within a substructure

Let $u_E(M, t)$ be the displacement field at any point M of Ω_E and at any time t of $[0, T]$, and let $\mathcal{U}^{[0,T]}$ be the associated space. $\varepsilon_E(M, t)$ is the strain field and the current state of the structure is characterized by the stress field $\sigma_E(M, t)$, whose associated space is $\mathcal{S}^{[0,T]}$. The mechanical problem to be solved within each substructure Ω_E is:

Find the evolutions of the displacement field $u_E(M, t)$ and stress field $\sigma_E(M, t)$ such that:

- Kinematic admissibility: $\forall t \in [O, T], u_E \in \mathcal{U}^{[0,T]}$
  · Initial conditions: $\forall M \in \Omega_E$

$$u_E(t = 0) = U_E^0 \qquad \frac{du_E}{dt}(t = 0) = V_E^0 \tag{1}$$

  · Boundary conditions: $\forall t \in [O, T], \forall M \in \Gamma_{EE'}$

$$\left.\frac{du_E}{dt}\right|_{\Gamma_{EE'}} = W_E \qquad u_E|_{\partial\Omega_1} = U_d \qquad F_E|_{\partial\Omega_2} = F_d \tag{2}$$

- Equilibrium: $\forall t \in [0, T], \forall \dot{u}^* \in U_0^{[0,T]}, \sigma_E \in \mathcal{S}^{[0,T]}$

$$\int_{\Omega_E} \left(\rho\frac{d^2 u_E}{dt^2} + f_d\right)\dot{u}^* d\Omega + \int_{\Omega_E} Tr\left(\sigma_E\varepsilon(\dot{u}^*)\right) d\Omega = \sum_{E'} \int_{\Gamma_{EE'}} F_{EE'}\dot{u}^* d\Gamma \tag{3}$$

- Elastic behavior: $\forall t \in [0, T], \forall M \in \Omega_E$

$$\sigma_E = \mathbf{K}_E\varepsilon(u_E) \tag{4}$$

where $\mathbf{K}_E$ is the Hooke's operator.

■ The problem at the interfaces

The mechanical problem to be solved at each interface $\Gamma_{EE'}$ is:

Find the evolutions of the force fields $F_E(M, t)$, $F_{E'}(M, t)$ and velocity fields $W_E(M, t)$, $W_{E'}(M, t)$ such that:
- General case: $\forall t \in [O, T], \forall M \in \Gamma_{EE'}$

$$(F_E, F_{E'}) = A_{\Gamma_{EE'}}(W_E, W_{E'}) \tag{5}$$

where the behavior is expressed as an evolution law $A_{\Gamma_{EE'}}$. Here, two examples of interface behavior are given.

- Perfect interface: The velocity is continuous at the interface and equilibrium is verified. The constitutive law is given by the relations:

$$F_E + F_{E'} = 0 \qquad \text{and} \qquad W_E - W_{E'} = 0 \tag{6}$$

- Unilateral contact with friction: The contact history must be taken into account during the loading in order for the friction conditions to be verified (34). A time discretization must be chosen. The interface displacement field U_E is introduced:

$$W_E^t = \frac{U_E^t - U_E^{t-\Delta t}}{\Delta t} = \frac{\Delta U_E^t}{\Delta t}$$

Let μ denote the friction coefficient, n_E the outward normal at a point of $\Gamma_{EE'}$, and g the initial gap (Figure 3). $\mathbf{P}_T$ is the tangential projector associated with Interface $\Gamma_{EE'}$ such that $W_E = (n_E.W_E)n_E + \mathbf{P}_T W_E$.
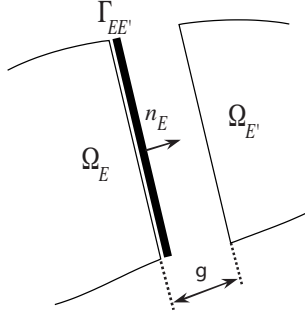

Fig. 3. A contact interface

The constitutive law (Equation 5) is described by the unilateral contact conditions:

$$\text{If } n_E \cdot (U_{E'}^t - U_E^t) + g > 0 \text{ then } F_E^t = F_{E'}^t = 0 \qquad \text{(separation)}$$

$$\text{If } n_E \cdot (U_{E'}^t - U_E^t) + g = 0 \text{ then } \begin{cases} F_E^t + F_{E'}^t = 0 \\ n_E \cdot F_E^t \leq 0 \end{cases} \qquad \text{(contact)}$$

and by the frictional conditions:

$$\text{If } \|\mathbf{P}_T F_E^t\| < \mu|n_E \cdot F_E^t| \text{ then } \mathbf{P}_T(W_{E'}^t - W_E^t) = 0 \qquad \text{(sticking)}$$

$$\text{If } \|\mathbf{P}_T F_E^t\| = \mu|n_E \cdot F_E^t| \text{ then } \begin{cases} \mathbf{P}_T(W_{E'}^t - W_E^t) \wedge \mathbf{P}_T F_E^t = 0 \\ \mathbf{P}_T(W_{E'}^t - W_E^t) \cdot \mathbf{P}_T F_E^t \geq 0 \end{cases} \qquad \text{(slipping)}$$

2.4 Resolution strategy: the LATIN method

The LATIN (LArge Time INcrement) method (35) is a general, mechanics-based computational strategy for the resolution of time-dependent nonlinear

6

problems which operates over the entire time-space domain. It has been applied successfully to a variety of problems (30; 36; 37; 38).

In the case of linear elastic substructures which is considered here, the solution $u_E(M,t)$, $\sigma_E(M,t)$ can be calculated from the boundary values $W_E(M,t)$, $F_E(M,t)$. Thus, a solution s is represented solely by the force and velocity fields on both sides of an interface. The solution of Problem s_{ref} is expressed as a set of time-dependent fields within each substructure and at the corresponding interfaces:

$$s_{ref} = \sum_E s_E \qquad s_E = \{F_E(M,t), W_E(M,t)\}$$

■ Separation of the difficulties

The LATIN approach is based on the idea of dealing with each difficulty separately in order not to have to solve a global problem and a nonlinear problem at the same time. The equations are divided into global linear equations and local nonlinear equations, so that $s_{ref} = A_d \cap \Gamma$ is the intersection of two subspaces:

- A_d, the space of the solutions of the linear equations associated with the substructures Ω_E: kinematic admissibility, equilibrium, elastic behavior and admissibility of the macroquantities;
- Γ, the space of the solutions of the local equations related to the interfaces $\Gamma_{EE'}$ and expressing their behavior.

■ A two-step iterative strategy

The LATIN method consists in seeking fields of Γ and A_d alternatively along two search directions E^+ and E^-, as shown in Figure 4. Each iteration involves two stages, called the local stage and the linear stage:

<u>Local stage:</u> Given $s_n = \{F_E, W_E\} \in A_d$, find $\widehat{s}_{n+1/2} = \{\widehat{F}_E, \widehat{W}_E\}$ such that:

$$\begin{aligned} \widehat{s}_{n+1/2} &\in \Gamma & \text{(interfaces)} \\ \widehat{s}_{n+1/2} - s_n &\in E^+ & \text{(search directions)} \end{aligned} \qquad (7)$$

<u>Linear stage:</u> Given $\widehat{s}_{n+1/2} = \{\widehat{F}_E, \widehat{W}_E\} \in \Gamma$, find $s_{n+1} = \{F_E, W_E\}$ such that:

$$\begin{aligned} s_{n+1} &\in A_d & \text{(substructures)} \\ s_{n+1} - \widehat{s}_{n+1/2} &\in E^- & \text{(search directions)} \end{aligned} \qquad (8)$$
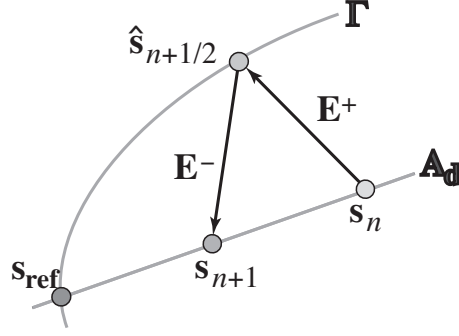
Fig. 4. An iteration of the LATIN method

In the case of linear elastic substructures which is considered here, the search directions are defined as follows:

$$\widehat{s}_{n+1/2} - s_n \in E^+ \Longleftrightarrow \widehat{F}_E - F_E = \mathbf{k}_0(\widehat{W}_E - W_E) \tag{9}$$

$$s_{n+1} - \widehat{s}_{n+1/2} \in E^- \Longleftrightarrow F_E - \widehat{F}_E = -\mathbf{k}_0(W_E - \widehat{W}_E) \tag{10}$$

where $\mathbf{k}_0$ is a scalar parameter of the method. As long as $\mathbf{k}_0$ remains positive, the solution of the problem does not depend on the value of this parameter, which affects only the convergence rate of the algorithm. For the dynamic cases being addressed here, the optimum value of $\mathbf{k}_0$ for a 1D problem was given in (38): $\mathbf{k}_0 = \sqrt{\rho E}$, where E is the Young's modulus and ρ the density. $\mathbf{k}_0$ can be viewed as a local impedance of the material. This parameter is very similar to the penalty term of the augmented Lagrangian method. However, in our case, the interfaces are discretized using finite elements. Consequently, for the 3D case, the force fields at the interfaces correspond to stress fields. Thus, one takes the same value of the parameter, *i.e.* $\sqrt{\rho E}$, for 1D, 2D and 3D cases. For an interface between two materials with different impedance, one takes the mean value.

An error indicator η is used to control the convergence of the algorithm toward s_{ref}. This indicator is a measure of the distance between the two solutions s_{n+1} and $\widehat{s}_{n+1/2}$:

$$\eta^2 = \frac{\sum_E \left\| s_{n+1} - \widehat{s}_{n+1/2} \right\|^2}{\sum_E \left\| s_{n+1} \right\|^2 + \sum_E \left\| \widehat{s}_{n+1/2} \right\|^2}$$

where:

$$\| s_{n+1} \|_E^2 = \int_0^T \int_{\partial\Omega_E} F_E^T \mathbf{k}_0^{-1} F_E + W_E^T \mathbf{k}_0 W_E \, dS dt$$

8

2.5   The local stage: $\widehat{s}_{n+1/2}$

The local stage consists in building $\widehat{s}_{n+1/2} \in \Gamma$ knowing $s_n \in Ad$. Then, $(\widehat{s}_{n+1/2} - s_n)$ must follow the search direction E^+ defined in Equation 9.

■ Perfect interface

Let us consider the case of a perfect interface $\Gamma_{E'E}$ between Substructures Ω_E and $\Omega_{E'}$. The unknowns are $(\widehat{W}_E, \widehat{W}_{E'}, \widehat{F}_E, \widehat{F}_{E'})$, which must verify the behavior equation (Equation 6) and follow the search direction E^+ (Equation 9). The solution of these equations is:

$$\widehat{W}_E = \widehat{W}_{E'} = \frac{1}{2}\Big[W_E + W_{E'} - \mathbf{k}_0^{-1}(F_E + F_{E'})\Big] \tag{11}$$

$$\widehat{F}_E = -\widehat{F}_{E'} = \frac{1}{2}\Big[F_E - F_{E'} - \mathbf{k}_0(W_E - W_{E'})\Big] \tag{12}$$

■ Contact interface with friction

For contact interfaces, the introduction of two indicators g_N and g_T (28; 30) enables one to obtain the contact status (separation, contact, sticking or slipping) explicitly. At each point of the interface, the normal contact indicator g_N for the current load step $t + \Delta t$ is given by:

$$g_N^{t+\Delta t} = \frac{1}{2}n_E.\Big(W_{E'}^{t+\Delta t} - W_E^{t+\Delta t} + \frac{\widehat{W}_{E'}^t - \widehat{W}_E^t}{\Delta t}\Big)$$
$$+ \frac{g}{2} - \frac{1}{2\mathbf{k}_0}n_E.(F_{E'}^{t+\Delta t} - F_E^{t+\Delta t}) \tag{13}$$

The non-penetration condition is expressed as: If $g_N^{t+\Delta t} > 0$, separation occurs; otherwise, contact occurs. Let us note that at load step $t + \Delta t$ the "hat" quantities with the superscript t are known.

The friction indicator g_T is defined by:

$$g_T^{t+\Delta t} = \frac{k}{2}\mathbf{P}_T(W_{E'}^{t+\Delta t} - W_E^{t+\Delta t}) - \frac{1}{2}\mathbf{P}_T(F_{E'}^{t+\Delta t} - F_E^{t+\Delta t}) \tag{14}$$

The frictional condition can be written as: If $g_T^{t+\Delta t} < \mu|n_E.\widehat{F}_E^t|$, slipping occurs; otherwise, sticking occurs. Finally, the normal and tangential components of the interface quantities $\widehat{W}_E^{t+\Delta t}$, $\widehat{W}_{E'}^{t+\Delta t}$, $\widehat{F}_E^{t+\Delta t}$ and $\widehat{F}_{E'}^{t+\Delta t}$ are determined according to the contact status.

2.6 The linear stage: s_{n+1}

The linear stage consists in building $s_{n+1} \in Ad$ knowing $\widehat{s}_{n+1/2} \in \Gamma$:

- Macroadmissibility: in order to ensure the admissibility conditions of the macro variables, we introduce Lagrange multipliers $\widetilde{W}_E^M$ at the interfaces.
- Search direction: the unknowns (W_E, F_E) must follow the search direction. Equation 10 must be modified by introducing the Lagrange multipliers defined at the interfaces. The new search direction E^- is defined as follows:

$$(F_E - \widehat{F}_E) + \mathbf{k}_0(W_E - \widehat{W}_E - \widetilde{W}_E^M) = 0 \tag{15}$$

- Equations associated with the substructures: the unknowns (W_E, F_E) must verify the dynamic equilibrium and the elastic behavior (Equations 3 and 4).

These equations lead to the resolution of an independent problem, called the "micro" problem, in each substructure:

Find $u_E(M,t)$, $\forall t \in [0,T], \forall \dot{u}^* \in U_0^{[0,T]}, \sigma_E \in \mathcal{S}^{[0,T]}$

$$\int_{\Omega_E} \left(\rho \frac{d^2 u_E}{dt^2} + f_d \right) \dot{u}^* d\Omega + \int_{\partial\Omega_E} \mathbf{k}_0 \frac{du_E}{dt} \dot{u}^* dS + \int_{\Omega_E} \mathbf{K}_E \varepsilon(u_E)\varepsilon(\dot{u}^*)d\Omega =$$

$$\sum_{E'} \int_{\Gamma_{EE'}} \left(\widehat{F}_E + \mathbf{k}_0 \widehat{W}_E + \mathbf{k}_0 \widetilde{W}_E^M \right) \dot{u}^* d\Gamma \tag{16}$$

■ Discretization

In each substructure, using a classical finite element discretization $u_E(M) = \{N\}^T\{U\}$ and $\varepsilon_E(M) = [B]\{U\}$, Equation 16 leads to the resolution of an evolution problem:

Find $U_t, \forall t \in [O, T]$ such that:

$$[M_E]\ddot{U}_t + [c_E]\dot{U}_t + [K_E]U_t = \widehat{F}_t + \mathbf{k}_0(\widehat{W}_t + \widetilde{W}_t^M) \tag{17}$$

where $[M_E]$ and $[K_E]$ are the classical finite element mass and stiffness matrices. Matrix $[c_E]$ is less classical and is specific to the LATIN method. These matrices are defined by:

$$
\begin{aligned}
M_E &= \int_{\Omega_E} \rho\{N\}^T\{N\}d\Omega \\
c_E &= \int_{\partial\Omega_E} \mathbf{k}_0\{N\}^T\{N\}dS \\
K_E &= \int_{\Omega_E} [B]\mathbf{K}_E[B]d\Omega
\end{aligned}
\tag{18}
$$

In order to solve the evolution problem 17, the finite element discretization must be associated with a time integration scheme. We chose to use the classical Newmark scheme:

$$
\begin{aligned}
\dot{U}_{t+\Delta t} &= \dot{U}_t + \Delta t\left((1-\gamma)\ddot{U}_t + \gamma\ddot{U}_{t+\Delta t}\right) \\
U_{t+\Delta t} &= U_t + \Delta t\dot{U}_t + \Delta t^2\left((1/2-\beta)\ddot{U}_t + \beta\ddot{U}_{t+\Delta t}\right)
\end{aligned}
\tag{19}
$$

For the numerical example, let $\gamma = 1/2$ and $\beta = 1/4$, which corresponds to a trapezoidal rule with constant mean acceleration.

Then, the linear system which needs to be solved at each time step takes the form:

$$
\left(\frac{1}{\gamma\Delta t}[M_E] + [c_E] + \frac{\beta\Delta t}{\gamma}[K_E]\right)\dot{U}_{t+\Delta t} = \widehat{F}_{t+\Delta t}
$$
$$
+ \mathbf{k}_0\left(\widehat{W}_{t+\Delta t} + \widetilde{W}^M_{t+\Delta t}\right) + f(t) \tag{20}
$$

where

$$
f(t) = -[K_E]U_t + \left(\frac{1}{\gamma\Delta t}[M_E] - \left(1-\frac{\beta}{\gamma}\right)\Delta t[K_E]\right)\dot{U}_t
$$
$$
+ \left(\left(1-\frac{1}{\gamma}\right)[M_E] - \left(\frac{1}{2}-\frac{\beta}{\gamma}\right)\Delta t^2[K_E]\right)\ddot{U}_t
$$

System 20 cannot be solved because there are two unknowns, $\dot{U}_{t+\Delta t}$ and $\widetilde{W}^M_{t+\Delta t}$. Therefore, one divides Field $\dot{U}$ into two fields, $\dot{U}^1$ and $\dot{U}^2$, such that $\dot{U} = \dot{U}^1 + \dot{U}^2$ and Fields $\dot{U}^1$ and $\dot{U}^2$ are solutions of the following two microproblems:

$$
\left(\frac{1}{\gamma\Delta t}[M_E] + [c_E] + \frac{\beta\Delta t}{\gamma}[K_E]\right)\dot{U}^1_{t+\Delta t} = \widehat{F}_{t+\Delta t} + \mathbf{k}_0\widehat{W}_{t+\Delta t} + f(t) \tag{21}
$$

$$
\left(\frac{1}{\gamma\Delta t}[M_E] + [c_E] + \frac{\beta\Delta t}{\gamma}[K_E]\right)\dot{U}^2_{t+\Delta t} = \mathbf{k}_0\widetilde{W}^M_{t+\Delta t} \tag{22}
$$

With this decomposition, Equation 21 can be easily solved after a local stage because fields $\widehat{F}_{t+\Delta t}$, $\widehat{W}_{t+\Delta t}$ and Function $f(t)$ are known. Equation 22 cannot be solved without one's knowledge of $\widetilde{W}^M$, but this problem can be easily inverted because of the very small number of degrees of freedom of $\widetilde{W}^M$ (nine DOFs per interface for a 3D problem), and one can write:

$$
W^{2,M} = \mathbf{L}_E^{-1}\widetilde{W}^M \tag{23}
$$

where $W^{2,M} = \Pi_{\Gamma_{EE'}}\dot{U}^2\big|_{\Gamma_{EE'}}$

$\mathbf{L}_E$ represents a condensation operator for Substructure Ω_E of Problem 22 on the coarse scale of the interfaces. These operators are calculated only once for all the substructures at the beginning of the algorithm: Problem 22 is solved for each value of $\widetilde{W}^M$ and the result at the interface is projected onto the coarse scale to obtain the corresponding value of $W^{2,M}$ (the macro part of the restriction of $\dot{U}^2$ to the interfaces).

The decomposition of Field $\dot{U}$ into $\dot{U}^1 + \dot{U}^2$ using the search direction (Equation 15) and the projector $\Pi_{\Gamma_{EE'}}$ involves some other relations for $W^{1,M}$ and $W^{2,M}$ (the macro parts of the restrictions of Fields $\dot{U}^1$ and $\dot{U}^2$ to the interfaces):

$$
\begin{aligned}
W^M &= W^{1,M} + W^{2,M} \\
F^{1,M} &- \widehat{F}^M + \mathbf{k}_0(W^{1,M} - \widehat{W}^M) = 0 \\
F^{2,M} &+ \mathbf{k}_0(W^{2,M} - \widetilde{W}^M) = 0
\end{aligned}
\tag{24}
$$

■ The macroproblem

The admissibility of the macroquantities at all the interfaces along with the condensation operator of all the substructures (Equation 23) lead to the definition of the macro problem.

In order to present the construction of the macroproblem, let us consider a perfect interface. The admissibility of the macroquantities at such an interface corresponds to the continuity of the macroscopic velocities and to the equilibrium of the macroscopic forces.

With such admissibility conditions, one must introduce two Lagrange multipliers per interface, as shown in Figure 5.
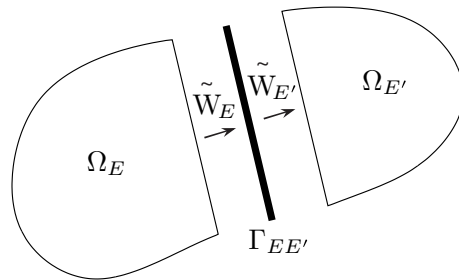

Fig. 5. Lagrange multipliers $\widetilde{W}_E^M$ and $\widetilde{W}_{E'}^M$ for a perfect interface

The contribution of the perfect interface $\Gamma_{EE'}$ to the macroproblem (Equations 25 and 26) is expressed through Equations 23, 24 and the admissibility conditions.

Continuity of the macroscopic velocities:

$$W_E^M = W_{E'}^M \quad \Longleftrightarrow$$

$$\begin{bmatrix} \mathbf{L}_E & -\mathbf{L}_{E'} \end{bmatrix} \begin{bmatrix} \widetilde{W}_E^M \\ \widetilde{W}_{E'}^M \end{bmatrix} = \begin{bmatrix} -W_E^{1,M} + W_{E'}^{1,M} \end{bmatrix} \qquad (25)$$

Equilibrium of the macroscopic forces:

$$F_E^M + F_{E'}^M = 0 \quad \Longleftrightarrow$$

$$\begin{bmatrix} \mathbf{k}_0(1 - \mathbf{L}_E) & \mathbf{k}_0(1 - \mathbf{L}_{E'}) \end{bmatrix} \begin{bmatrix} \widetilde{W}_E^M \\ \widetilde{W}_{E'}^M \end{bmatrix} = \begin{bmatrix} -F_E^{1,M} - F_{E'}^{1,M} \end{bmatrix} \qquad (26)$$

The quantity $\widetilde{W}_E^M$ is a vector which contains all the Lagrange multipliers of Substructure Ω_E. Thus, this problem couples all the macro variables of the entire structure and enables the Lagrange multiplier $\widetilde{W}_E^M$ to be defined for all the substructures. $W_E^{1,M}$ is the macro part of the solution of the first microproblem (Equation 21); $F_E^{1,M}$ is calculated using the search direction (Equation 24).

■ Comparison with the coarse problem introduced by Farhat-Shen-Mandel

In (11), the introduction of the coarse problem into the FETI method for the dynamic case enables a specific rigid body motion to be applied to each floating subdomain in order to reposition this subdomain *globally* at the beginning of each iteration. The evaluation of the rigid body correction is carried out in a projection step. This problem couples all of the subdomain rigid body corrections. For the 3D case, its size is, at the most, $6N_f \times 6N_f$, N_f being the number of floating subdomains. Once the floating subdomains have been positioned globally, the *local* corrections are calculated using a PCPG algorithm.

In that approach as in ours, the coarse problem leads to the scalability of the iterative strategy. The main difference concerns the coarse space. In (11), the coarse space consists of the rigid body motions of all floating subdomains. In our approach, the scale separation is performed at the interfaces and the coarse space consists of the linear parts of the interface fields. We enforce continuity of the velocities and equilibrium of the forces in the macro parts. The macroproblem is somewhat larger in our case: $(2 \times 9N_p) \times (2 \times 9N_p)$ for the 3D case, N_p being the number of perfect interfaces.

The LATIN method associated with the mixed domain decomposition method is inherently parallelizable (34). In our case, this strategy was programmed in C++ in the framework of the finite element platform developed by H. Leclerc (39). Libraries such as MPI (Message Passing Interface) for the transfer of information among machines were used in order to be able to use PC-cluster types of architectures. In order to parallelize the strategy, the first step is to allocate the substructures and interfaces among the different processors. This is done through the METIS libraries (40), which enable the number of data which must circulate among the processors to be minimized in order not to result in an excessive decline in speedup. Then, the different operators specific to the substructures are constructed on each processor. During the iterative resolution phase, the first and second microproblems are solved simultaneously. The macroproblem, which has not been parallelized yet, is solved on a single processor. Finally, the local stage is completely parallelized because the interfaces are distributed among the different processors.

- Linear stage
Loop over time ($\forall t \in [0, T]$)
- Loop over the substructures (on each processor):
  First microproblem: determination of $(\dot{U}_E^1, W_E^1)$ given $(\widehat{W}_E, \widehat{F}_E)$ (Equation 21). Calculation of $W_E^{1,M} = \Pi_{\gamma_{EE'}} W_E^1$, then $F_E^{1,M}$, using the search direction and the admissibility conditions of the macro-quantities.
- Macroproblem (on a single processor):
  Determination of $\widetilde{W}_E^M$ given $W_E^{1,M}$ and $F_E^{1,M}$ (Equations 25, 26)
- Loop over the substructures (on each processor):
  Second microproblem: Determination of $(\dot{U}_E^2, W_E^2)$ given $\widetilde{W}_E^M$ (Equation 22)
Calculation of $\dot{U}_E = \dot{U}_E^1 + \dot{U}_E^2$ at time step t
End Loop

- Local stage
Loop over time ($\forall t \in [0, T]$)
- Loop over the interfaces (on each processor):
  Determination of $(\widehat{W}_E, \widehat{F}_E)$ given (W_E, F_E) (Equations 11, 12)
End Loop
Iteration until convergence

Algorithm 1. The micro/macro LATIN method (velocity approach)

The LATIN method consists in perform linear stages and local stages alternatively. The iterations concern the whole time interval, *i.e.* a solution over

the whole time interval is calculated at each iteration of the method. In the linear stage, an incremental formulation is used to solve problems within the substructures over the whole time interval. Thus, only two time steps of a substructure's fields (displacement, velocity and acceleration) need to be stored: the current time step being calculated and the previous time step. However, the interface quantities $(\widehat{F}, \widehat{W}, F, W)$ must be stored over the whole time interval. The fields are saved during the last iteration of the method for post-processing purposes. Algorithm 1 shows the key steps of an iteration of the multiscale method.

3   Numerical examples

3.1   3D linear academic problem

In order to test the method described previously, let us consider the simple 3D example of the propagation of a compression wave in a bar composed of two parallelepipeds (Figure 6). The bar is 1 m long and 0.25 m wide, with Young's modulus 200 GPa, mass density 7,800 kg/m^3 and Poisson's ratio 0.3. The loading consists in a prescribed velocity going from 0 m/s initially to a maximum value of 1 m/s over a period T of 60 μs. For the purpose of this test, each parallelepiped can be decomposed into several substructures. The interface between the two parallelepipeds can be perfect or can involve frictional contact.
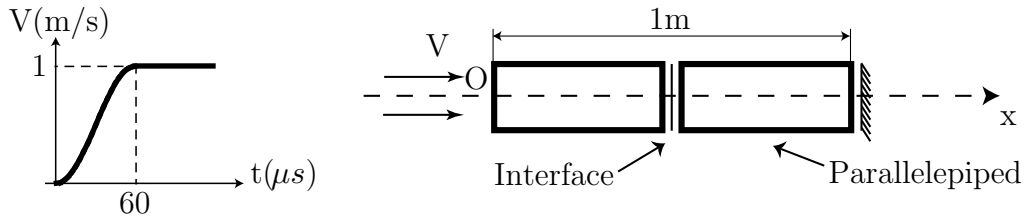

Fig. 6. The numerical example

The purpose of the test was to evaluate the efficiency of the multiscale method. In order to do that, we assumed a perfect interface between the two parallelepipeds and decomposed each parallelepiped into 2 substructures. Figure 7 shows the mesh used for the test, which contains about 5,600 DOFs. We used 79 time steps of 5 μs each for a total duration of 395 μs.
 Figure 8 shows the velocity field along the (O, x) axis (defined in Figure 6) as a function of time. The result of the multiscale LATIN method is compared with that of the single-scale LATIN method (37). The single-scale LATIN method is similar to the method developed here except that there is no macroproblem. Using the single-scale method (Figures 8(a), 8(b) and 8(c)), several iterations

15

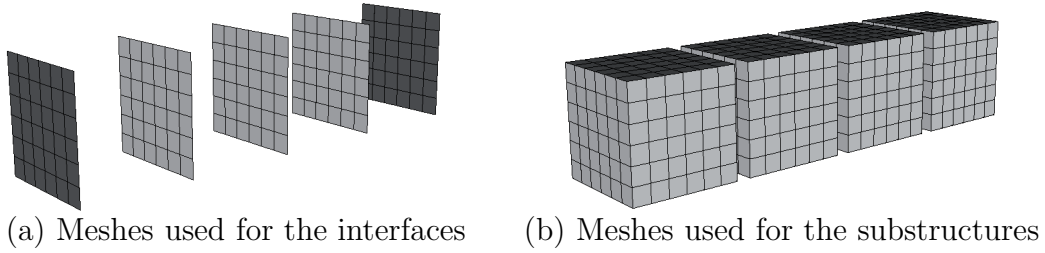(a) Meshes used for the interfaces   (b) Meshes used for the substructures

Fig. 7. The meshes used for the example

are necessary for the wave to propagate throughout the structure. With the multiscale method (Figure 8(d)), the first iteration gives a good approximation of the solution, thanks to the macroproblem which provides a representation of the macroscopic part of the solution.
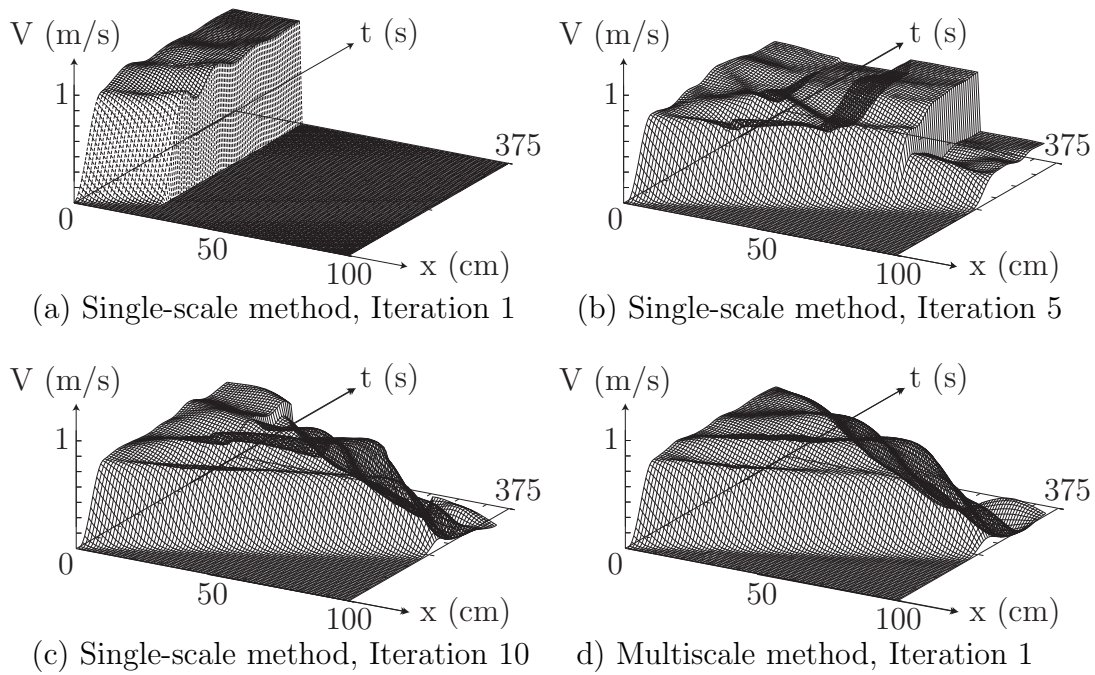

(a) Single-scale method, Iteration 1   (b) Single-scale method, Iteration 5

(c) Single-scale method, Iteration 10   d) Multiscale method, Iteration 1

Fig. 8. Evolution of the velocity field V along the (O, x) axis (m/s) as a function of time (μs) and x (cm)

3.2 Scalability and speedup

In order to illustrate the convergence of the multiscale LATIN method, let us consider the same example as in Figure 6, but use a finer mesh which enables us to decompose the two parallelepipeds into 4, 12 or 24 substructures. Figure 9 shows the convergence rate of the multiscale method for each decomposition. The multiscale approach is scalable: the convergence rate does not depend on the number of substructures.
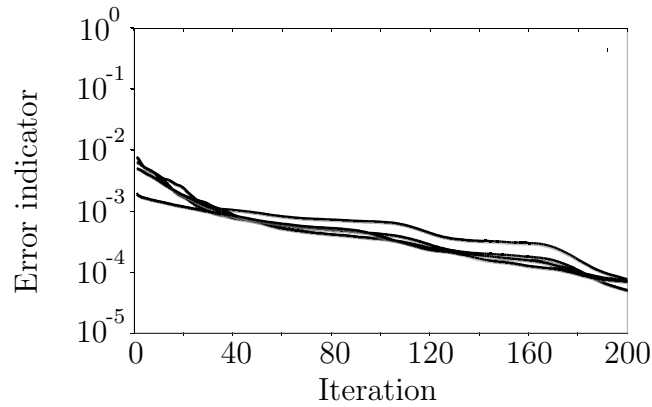
16

Fig. 9. Convergence rate of the multiscale method

The efficiency of the multiscale method is illustrated by the rate of evolution of the error indicator during the process. Figure 10 shows the convergence rate of the single-scale method using 4, 12 and 24 substructures along with that of the multiscale method. These curves show that the convergence rate of the single-scale method is highly dependent on the number of substructures and that the convergence rate of the multiscale method is better than that of the single-scale method.
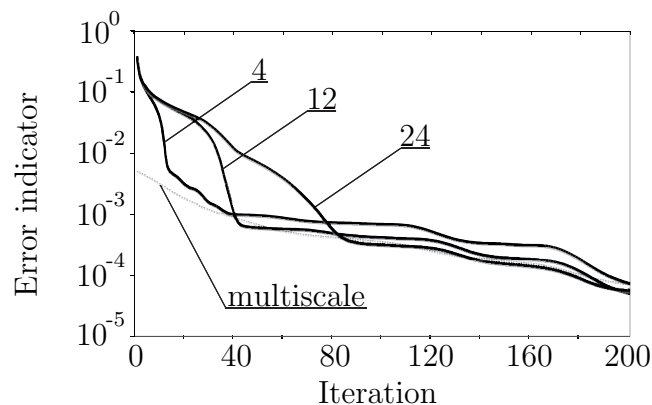

Fig. 10. The convergence rate of the single-scale method

Figure 11 shows the speedup of the parallel algorithm obtained with the previous example of Figure 6. For this application, we used a 150,000-DOF mesh decomposed into 144 substructures of 1,000 DOFs each.

With a small number of processors, the speedup is very good because the calculation of the macroproblem and the data exchanges among the processors are negligible compared to the calculation of the two microproblems. This is no longer true when the number of processors increases. Moreover, the macroproblem is not parallelized and, therefore, as the number of processors increases the macroproblem becomes more and more significant compared to the microproblem.
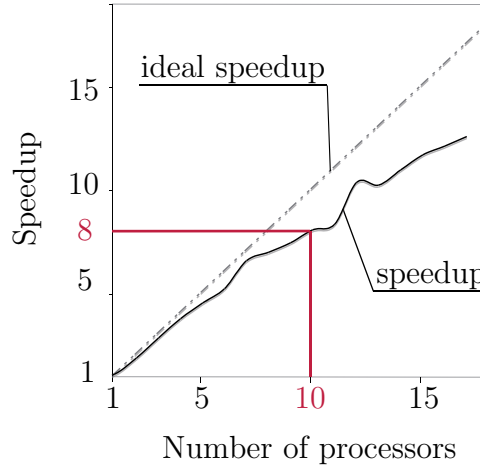
17

Fig. 11. Speedup of the academic example

3.3 Frictional contact with gap

The objective of this section is to show that the multiscale LATIN method is indeed capable of carrying out nonlinear calculations such as frictional contact. In order to do that, let us consider the same example of two parallelepipeds, this time with a gap of initially 40-μm and a frictional contact interface with a friction coefficient of 0.3. The gap between the two parallelepipeds creates a shock wave when they come in contact. We analyzed this problem with both the multiscale LATIN method and the finite element code LS-DYNA3D, using the same mesh in both cases.

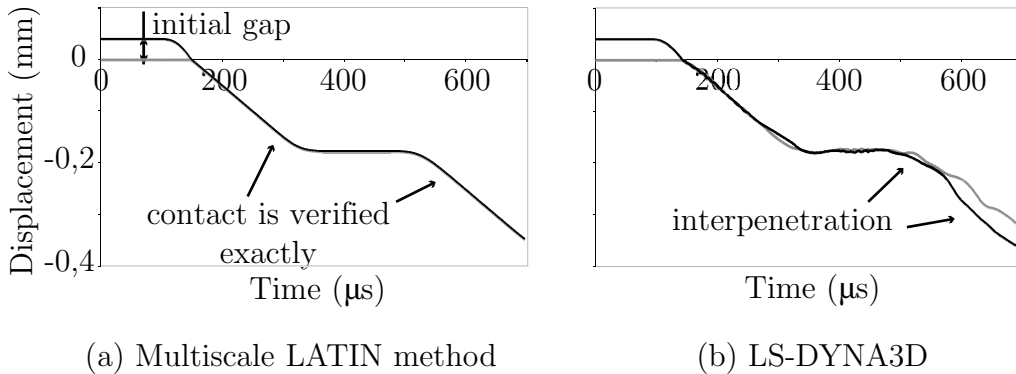(a) Multiscale LATIN method   (b) LS-DYNA3D

Fig. 12. Displacement of a point on either side of the interface as a function of time

Figure 12 shows the displacement of a point on either side of the interface as a function of time. In the result obtained with the multiscale LATIN method (Figure 12(a)), the behavior of the interface is verified: the gap can be observed at the beginning of the curve; then, the two parallelepipeds come into contact. In the result obtained with LS-DYNA3D (Figure 12(b)), the behavior of the interface is not verified exactly. One can see that at times the two parallelepipeds are not in contact as they should be, and that they interpenetrate at

the end of the calculation. These results show that, contrary to LS-DYNA3D, the multiscale LATIN method is suitable for studying the influence of the friction coefficient on the solution.

Figure 13 shows the evolution of the error indicator for problems with frictional contact, contact without friction and without contact (perfect interface). This curve shows that the convergence rates for problems with contact with and without friction are the same. Moreover, the comparison of this curve with the convergence rate for problem without contact shows that there is a difference, but that it is small.
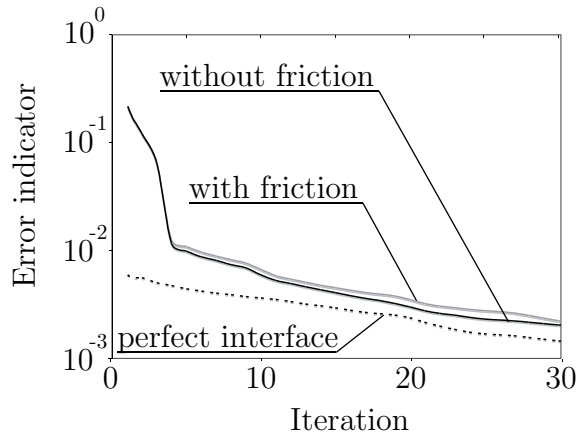

Fig. 13. Speedup of the academic example

3.4 Application to a 3D heterogenous material

This example concerns the propagation of a compression or traction wave in a 3D heterogenous material composed of a matrix and several grains of different sizes (Figure 14)(c). There is frictional contact at the interfaces between the grains and the matrix. The friction coefficient is equal to 0.3. The Young's modulus of the grains is 200 GPa, their mass density 7,800 kg/m^3 and their Poisson's ratio 0.3. The Young's modulus of the matrix is 50 GPa, its mass density 7,800 kg/m^3 and its Poisson's ratio 0.2. These choices enable us to have different wave velocities in the materials and also to have both reflection and propagation when a compression wave reaches a grain/matrix interface. The loading consists of a prescribed velocity as shown in Figure 14 ($V_{max} = 1$ m/s).

In order to deal with this problem, we decomposed the matrix into several substructures. Figure 14(a) shows the 3D mesh used for one cell. This decomposition led to a good speedup of the parallel algorithm. We used 64 elementary cells of 60,000 DOFs each. Each cell was divided into 7 substructures, for a total of 448 substructures and 1,326 interfaces, including 384 frictional con-
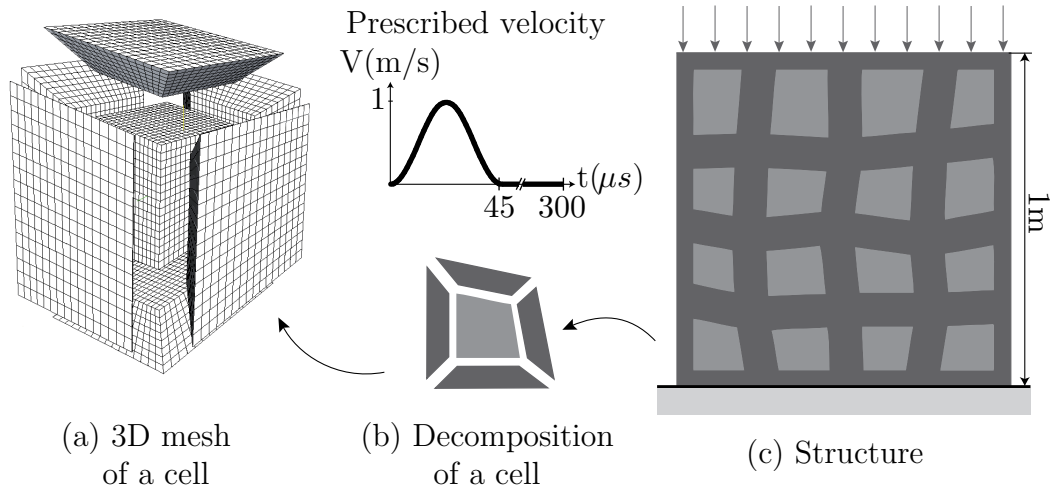
19

Fig. 14. Composition of the heterogenous material

tact interfaces. The direct resolution of this problem would involve 3,840,000 DOFs. For this example, we used an implicit scheme for the time integration with 99 time steps of 3 μs each for a total duration of 300 μs.

We used a PC cluster of 48 processors to carry out this simulation. These calculations took 15 hours (150 iterations). Figure 15(a) shows the velocity fields obtained at time step 20 for a compression wave. The left-hand side shows the velocity field on the external skin of the structure. The right-hand side shows the velocity field inside the structure, in a plane going across the grains. One can observe the progression of the wave within the grain and the discontinuity of the velocity between the grain and the matrix. Figure 15(b) shows the displacement field at time step 40 for a compression wave. Here, one can observe the separation of the matrix from the grain.
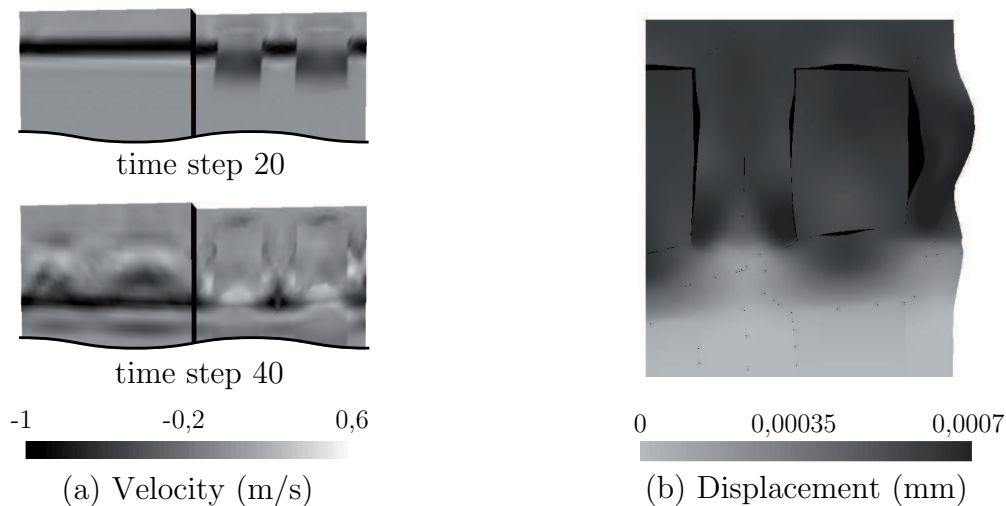

Fig. 15. Results of the calculation

4 Conclusion

We presented the extension of the multiscale LATIN method to dynamic problems for complex 3D structural assemblies. As had already been proven in statics, the multiscale method marks a significant improvement compared to the single-scale method. The multiscale approach leads to the scalability of the method and a better convergence rate.

Our approach is based on two components: a mixed decomposition of the structure which provides significant modularity to the problem description, and an iterative resolution scheme. Compared to other commercial finite element tools, this method is particularly well-suited for the study of problems with frictional contact. The strategy is also fully parallelized. Its implementation into a cluster architecture leads to good behavior of the parallel algorithm and enables one to treat complex real-life structural assemblies with very large numbers of degrees of freedom.

The next step will be the application of this strategy to larger 3D assemblies, taking into account variations of the the friction coefficient. The multiscale LATIN method enables one to reuse the solution of a problem in order to solve similar problems. This strategy has already been applied successfully to a variety of static problems (41) and is an efficient strategy for the parametric analysis of problems with multiple contacts.

References

[1] J.O. Hallquist, G.L. Goudreau and D.J. Benson, *"Sliding interfaces with contact-impact in large-scale lagrangien computations"*. Computer Methods in Applied Mechanics and Engineering, 51, 107-137, 1985.

[2] M. Barboteu, P. Alart, and M. Vidrascu, *" A domain decomposition strategy for nonclassical frictional multi-contact problems."*. Computer Methods in Applied Mechanics and Engineering, 190:4785–4803, 2001.

[3] P. Alart, M. Barboteu, P. Le Tallec, and M. Vidrascu, *" Méhode de scharwz additive avec solveur grossier pour problemes non symetriques."*, Comptes-Rendus de l'AcadÈmie des Sciences de Paris, 331:399–404, 2000.

[4] C. Farhat and F.-X. Roux, *"A method of nite element tearing and interconnecting and its parallel solution algorithm."*, Int Jal for Numerical Methods in Engineering, 32, 1205-27, 1991.

[5] C. Farhat, L. Crivelli and F.-X. Roux, *"A transient FETI methodology for large-scale parallel implicit computations in structural mechanics"*, Int Jal for Numerical Methods in Engineering, 37, 1945-75, 1994.

[6] C. Farhat and F.-X. Roux, *"Implicit parallel processing in structural me-

chanics", Computer Methods in Applied Mechanics and Engineering, 2, 1-124, 1994.

[7] Z. Dostal, F. G. Neto, and S. Santos, *" Solution of contact problems by feti domain decomposition with natural coarse space projection."*, Computer Methods in Applied Mechanics and Engineering, 190(13-14):1611–1627, 2000.

[8] D. Dureisseix and C. Farhat, *" A numerically scalable domain decomposition method for solution of frictionless contact problems."*, International Journal for Numerical Methods in Engineering, 50(12):2643–2666, 2001.

[9] C. Farhat and J. Mandel, *"The two-level FETI method for static and dynamic plate problems"*, Computer Methods in Applied Mechanics and Engineering, 555, 129-151, 1998.

[10] C. Farhat, M. Lesoinne and K. Pierson, *"A scalable dual-primal domain decomposition method"*, Numer. Lin. Alg. Appl., 7, 687-714, 2000.

[11] C. Farhat, P.-S. Chen and J. Mandel, *"A scalable Lagrange multiplier based domain decomposition method for time-dependent problems"*, Int Jal for Numerical Methods in Engineering, 38, 3831-53, 1995.

[12] M. Barboteu, *" Construction du preconditionneur neumann-neumann de decomposition de domaine de niveau 2 pour des problemes elastodynamiques en grandes deformations."*, Comptes-Rendus de l'AcadÈmie des Sciences de Paris, 340:171–176, 2005.

[13] A. Gravouil and A. Combescure, *"Multi-time-step and two-scale domain decomposition method for non-linear structural dynamics"*, Int Jal for Numerical Methods in Engineering, 58, 1545-69, 2003.

[14] I.D. Parsons and JF. Hall, *"The multigrid method in solids mechanics: part Ialgorithm description and behaviour"*, Int Jal for Numerical Methods in Engineering, 29, 719-37, 1990.

[15] N. Kikuchi and J.T. Oden, *"Contact problems in elasticity: a study of variational inequalities and finite element methods"*, SIAM, Philadelphia, 1988.

[16] Z. Zhong and J. Mackerle, *"Static contact problems : a review"*, Engineering Computations, 9, 3-37, 1992.

[17] P. Wriggers, *"Finite element algorithms for contact problems"*, Archives of Computational Methods in Engineering, 2, 1-49, 1995.

[18] P. Wriggers and al., *"Penalty and augmented Lagrangian formulations for contact problems"*, Proc. NUMETA Conf., Swansea, 1985.

[19] N. Kikuchi, *"Penalty/nite element approximations of a class of unilateral contact problems"*, In Penalty method and nite element method, ASME, New York, 1982.

[20] F. Armero and E. Petcz, *"Formulation and analysis of conserving algorithms for dynamic contact / impact problems"*, Computer Methods in Applied Mechanics and Engineering, 158, 269-300, 1998.

[21] P. Alart and A. Curnier, *"A mixed formulation for frictional contact problems prone to Newton like solution methods"*, Computer Methods in Applied Mechanics and Engineering, 92, 253-375, 1991.

[22] J.S. Arora, A.I. Chahande and J.K. Paeng, *"Multiplier methods for engineering optimization"*, Int Jal for Numerical Methods in Engineering, 32, 1485-1525, 1991

[23] A. Klarbring, *"Mathematical programming and augmented lagrangian methods for frictional contact problems"*, Proceedings of the Contact Mechanics International Symposium, Curnier A. (ed.), Presses Polytechniques et Universitaires Romandes, 409-422, 1992.

[24] B. Rabi, O. Baba and J.C. Gelin, *"Treatment of the frictional contact via a Lagrangian formulation."*, Mathematical and Computer Modelling, Rodin E.Y., Shillor M. (Eds.), Pergamon Press: Oxford, 28, 407-412, 1998.

[25] P. Chabrand, F. Dubois and M. Raous, *"Various numerical methods for solving unilateral contact problems with friction."*, Mathematical and Computer Modelling, Rodin E.Y., Shillor M. (Eds.), Pergamon Press: Oxford, 28, 97-108, 1998.

[26] K.J. Arrow, L. Hurwicz and H. Uzawa, *"Studies in nonlinear programming."*, University Press, Stanford, CA, 1958.

[27] J.C. Simo and T.A. Laursen, *"An augmented lagrangian treatment of contact problems involving friction."*, Computers and Structures, 42, 97-116, 1992.

[28] L. Champaney, J.-Y. Cognard and P. Ladevze, *"Modular analysis of assemblages of three-dimensional structures with unilateral contact conditions."*, Computers and Structures, 73, 249-266, 1999.

[29] P. Ladevèze and D. Dureissex, *"A micro/macro approach for parallel computing of heterogeneous structures"*. Int Jal for Computational Civil and Structural Engineering, 1, 1828, 2000.

[30] P. Ladevèze, A. Nouy and O. Loiseau, *"A multiscale computational approach for contact problems"*, Computer Methods in Applied Mechanics and Engineering Sofware, 191, 4869-4891, 2002.

[31] P. Lions, *" On the schwarz alternating method iii. a variant for non-overlapping subdomains."*, In Proceedings of Domain Decomposition Methods for Partial Differential Equations, 1990.

[32] R. Glowinski and P. Le Tallec, *" Augmented lagrangian interpretation of the nonoverlapping schwartz alternating method."*, In Internationnal Symposium on Domain Decomposition Methods, 224–231. Philadelphia, SIAM, 1990.

[33] P. Ladevèze, O. Loiseau and D. Dureissex, *"A micro-macro and parallel computational strategy for highly heterogeneous structures"*. Int Jal for Numerical Methods in Engineering, 52, 121-138, 2001.

[34] L. Champaney, J.Y. Cognard, D. Dureisseix and P. Ladevèze, *"Large scale applications on parallel computers of a mixed domain decomposition method."*, Computational Mechanics, 19, 253-263, 1997.

[35] P. Ladevèze, *"Nonlinear computational structural mechanics – New approaches and non-incremental methods of calculation"*, Springer-Verlag, 1999.

[36] P. Ladevèze and A. Nouy, *"On a multiscale computational strategy with*

time and space homogenization for structural mechanics", Computer Methods in Applied Mechanics and Engineering, 192, 3061-3087, 2003.

[37] P.A. Boucard, P. Ladevèze and H. Lemoussu, *"A modular approach to 3D impact computation with frictional contact"*, Computer & Structures, 78, 45-52, 2000.

[38] H. Lemoussu, P.A. Boucard and P. Ladevèze, *"A 3D shock computational strategy for real assembly and shock attenuator"*, Adv. Engrg. Software, 33, 517-526, 2002.

[39] H. Leclerc, *"Outil d'assistance au développement d'application d'analyse numérique et de mécanique"*, Séminaire du LMT Cachan, 2005.

[40] G. Karypsis and V. Kumar, *"METIS"*, A Software Package for Partitioning Unstructured Graphs, Partitioning Meshes, and Computing Fill-Reducing Orderings of Sparse Matrices, Version 4.0, Department of Computer Science, University of Minnesota, 1998.

[41] P.A. Boucard and L. Champaney, *"A suitable computational strategy for the parametric analysis of problems with multiple contact"*. Int Jal for Numerical Methods in Engineering, 57, 1259-1282, 2003.